Open access • Journal Article • DOI:10.1109/TSG.2017.2651030

Voltage Management for Large Scale PV Integration into Weak Distribution Systems

Licheng Wang, Ruifeng Yan, Tapan Kumar Saha

Institutions: University of Queensland

Published on: 01 Sep 2018 - IEEE Transactions on Smart Grid (Institute of Electrical and Electronics Engineers (IEEE))

Topics: Voltage regulation, Voltage optimisation, Voltage droop, Grid-connected photovoltaic power system and Volt-ampere reactive

Voltage Management for Large Scale PV Integration into Weak Distribution Systems

Licheng Wang, *Student Member, IEEE*, Ruifeng Yan, *Member, IEEE*, Tapan Kumar Saha, *Senior Member, IEEE*

***Abstract*--In long distribution feeders, Step Voltage Regulators (SVRs) with the Line Drop Compensation (LDC) have been widely implemented to control voltage profiles. After integration of photovoltaic (PV) systems, reactive power support from PV inverters can also be utilized in voltage regulation. Although both SVR and reactive power support can be effective to manage system voltage without coordination, problems such as large voltage variations and excessive SVR tap operations still exist in some strong PV power fluctuating days. In order to solve these issues, SVR and reactive power support should be assigned to different voltage regulation tasks according to their voltage regulation characteristics. Specifically, in a distribution system, an SVR should mainly deal with slowly changing quantities (*e.g.* load, upstream voltage), while the limited reactive power support should be used to counter fast fluctuating PV power. In this paper, the power factor droop parameters applied on PV inverters are optimally selected to achieve such coordination, so that voltage problems and excessive SVR tap operations can be successfully mitigated. The effectiveness of the proposed method is demonstrated via case studies. Future PV integration project in weak distribution systems can benefit from the innovative and practical methodology proposed in this paper.**

***Index Terms*--photovoltaic (PV), reactive power, power factor droop curve, coordination, optimization, distribution systems.**

I. Introduction

LARGE variations in photovoltaic (PV) generation can be caused by fast moving clouds [1], which can easily lead to serious voltage fluctuations in distribution systems. Traditionally, if On-Load Tap-Changer (OLTC) transformers or Step Voltage Regulators (SVRs) are properly set, they can successfully control the system voltage. However, as the PV penetration increases, new challenges (*e.g.* large voltage fluctuations, excessive SVR tap changes) arise [2, 3]. So far, a variety of voltage regulation methods have been proposed to solve these challenges. Most of these methods belong to reactive power support schemes.

Some optimal power flow (OPF) methods have been reported to optimally control reactive power support in voltage regulation. Centralized OPF problems are formulated in [4-7] to coordinate all the voltage regulation devices in power systems and provide optimal reactive power set points in different time-scales (hourly or 15-minute intervals). Different from the centralized OPF methods, distributed OPF algorithms [8, 9] can decompose an overall optimization problem into small sub problems and solve them in parallel. However, full observability of the whole power system in real time is needed in these OPF based methods, which are usually impractical especially in distribution systems. In addition, considering fast fluctuations of PV power due to the cloud transient effect, computation speed is another concern. The results from OPF methods may not be regarded as optimum any longer if large PV power has been changed during the computation intervals.

Compared with the OPF based methods, local reactive power control with predefined parameters are more popular in real life applications. These methods have fast response speed and can be easily implemented. In [10], a reactive power(voltage) - Q(V) droop curve is used for local voltage regulation in a 9.4MWp photovoltaic plant, which is connected to a transmission system in Romania. Moreover, power factor (PF) set point can be given by the PV plant operators to control the reactive power output. In [11], a reactive power(active power) - Q(P) curve is proposed using the German Grid Codes (GGC) to improve voltage profiles through reactive power support from PV inverters. On the basis of the GGC, a modified Q(P) curve is developed in [12], where a voltage sensitivity matrix is utilized to coordinate all the PV inverters in a distribution system with only local measurements. According to the analysis in [13], for voltage regulation, Q(V) control can have better performance compared with Q(P) control. In [14, 15], different reactive power compensation methods are compared, and allowable PV hosting capacities are estimated. A piecewise Q(P) curve is proposed in [16], whose parameters can be updated through a central optimization processor every 15 minutes. However, so far, few investigations have been reported considering the coordination between reactive power support and existing voltage regulation devices (*e.g.* SVRs).

In real life applications, there is indeed a need for such coordination. For the PV project of the University of Queensland (UQ) Gatton campus, a new established 3.15MWp PV plant is integrated into a weak distribution system, where an SVR is used to regulate the voltage profile. According to the Negotiated Customer Connection Contract [17], the PV plant power factor should always be within the range from 0.9 inductive to 0.9 capacitive. Therefore, a predefined power factor droop curve, namely PF(V) curve, is applied to provide reactive power support [18] in this PV plant. As shown in Fig. 1, the power factor of the PV plant

Corresponding author Ruifeng Yan is with the Global Change Institute, The University of Queensland, Brisbane, QLD 4072, Australia (e-mail: ruifeng@itee.uq.edu.au).

Licheng Wang and Tapan Kumar Saha are with the School of Information Technology and Electrical Engineering, The University of Queensland, Brisbane, QLD 4072, Australia (e-mail: l.wang8@uq.edu.au, saha@itee.uq.edu.au).

will vary according to its connection point voltage. Consequently, the PV plant can adaptively adjust its reactive power generation with local voltage, while remains its power factor within an allowable range (0.9 inductive to 0.9 capacitive). However, four parameters (V_{low}, V_{m1}, V_{m2}, V_{high}) of this PF(V) curve are empirically selected currently (0.96pu, 0.98pu, 0.996pu and 1.01pu), which may not coordinate well with the existing upstream SVR. As a result, excessive SVR tap operations and significant voltage variations may occur in large PV power fluctuating days.

The main contribution of this paper lies in the optimal selection of power factor droop parameters for the PV plant based on a novel approach of using the proposed voltage-PV generation curve. Under such development, the inverter reactive power support can be well coordinated with the existing SVR without the need of communication. Specifically, with this coordination established by the proposed method, limited reactive power support restricted by power factor (0.9 leading to 0.9 lagging) is properly utilized to counter strong PV power fluctuations, while SVR is only used to compensate slow changing quantities as it was originally designed. As a result, the issues of serious voltage variations and excessive SVR tap changes can be successfully alleviated in strong PV power fluctuating days. Future large scale PV integration projects in weak distribution systems can benefit from the valuable experience obtained in this research.

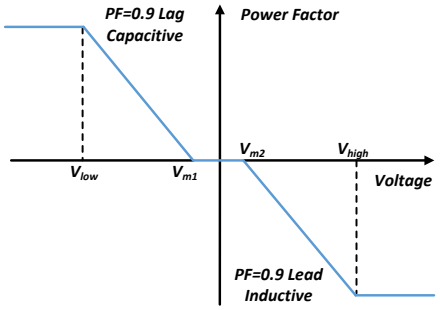

Fig. 1 Power factor droop curve.

II. Background Description

A. Investigated System

The UQ Gatton Campus is located in a fringe of the grid, which is expensive to upgrade. As in a rural area, the large scale PV plant can easily gain access to the low price land, but at the same time, it has to face the voltage regulation challenges in such a weak distribution network. The real Gatton distribution system topology is shown in Fig. 2, in which the 11kV feeder forks to two directions at the Point A after around 3km away from the Gatton zone substation. These two sub feeders are regulated by SVR A and SVR B respectively. The newly established 3.15MWp PV plant is connected at the end of the sub feeder that is regulated by SVR A. Replacing the sub feeder with SVR B by an equivalent load, the Gatton distribution system can be simplified as Fig. 3. In this distribution system, except for the existing SVR, reactive power support from the PV plant also can be utilized in voltage regulation. The power factor of this PV plant is limited within the range from 0.9 inductive to 0.9 capacitive by the local utility [17, 18].

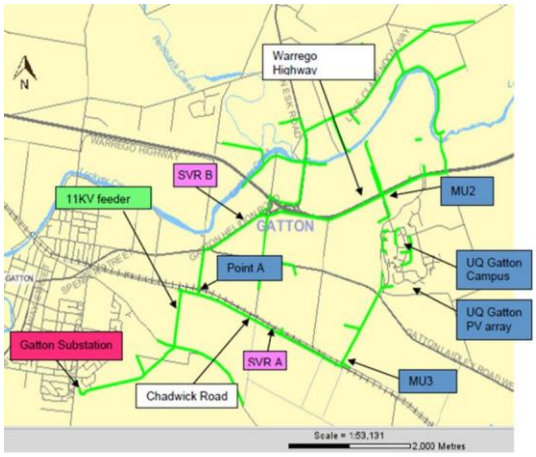

Fig. 2 Map of Gatton Campus of the University of Queensland [3].

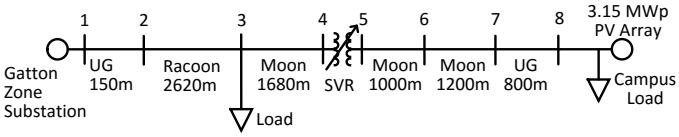

Fig. 3 Schematic figure of the 11kV Gatton network [3].

B. Problem Description

PV generation profile can be different from day to day due to variable weather conditions. The daily variability index (DVI) is adopted as in (1) to quantitatively describe the extent of PV power fluctuations [19]. As in Fig. 4, large DVI values are corresponding to days with strong PV power fluctuations, while small DVI values imply PV power fluctuations are insignificant.

$$DVI = \frac{Length\ of\ measured\ irradiance\ plot}{Length\ of\ clear\ sky\ irradiance\ plot} \quad (1)$$

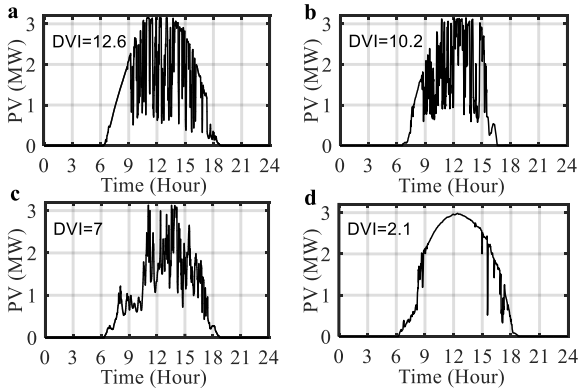

Fig. 4 PV power profiles with different DVI.

Before the PV plant was integrated into this distribution system, no serious voltage fluctuation existed under the regulation of the SVR. After integration of the PV plant, the SVR and PV inverters equipped with the power factor droop curve (Fig. 1) can still successfully regulate the PV connection point voltage for the majority of days. However, this power factor droop curve with empirically selected parameters and the independently running SVR cannot effectively control voltage variations during the days with large DVIs. For example, October 16th, 2015 (DVI =11.3) is a typical day with

strong PV power fluctuations. Under the regulation of the SVR and the reactive power support, the amount of relative voltage variations larger than 1.6%, 1.3%, 1.0%, 0.8% during that day were 8, 18, 37, 57 respectively, which exceed the maximum allowable occurrences of the perceptibility standard as in Table I [20]. The relative voltage variation is defined as the ratio of voltage deviation between consecutive measurements (with a resolution of one minute) to its nominal value. For example, $V(t)$ and $V(t+1)$ are two consecutive measurements, and the relative voltage variation ΔV can be expressed as

$$\Delta V = \frac{|V(t+1)-V(t)|}{V_n} \quad (2)$$

where V_n represents nominal value of the voltage. In addition, the total amount of SVR tap operations during this day was as high as 50 times, which implies SVR tap operations can be frequently triggered by large PV power fluctuations.

Fig. 5 shows the DVI distribution in October, 2015 (data available for 29 days), where PV power fluctuating levels are classified as serious, moderate and mild according to the levels of DVI. As in Fig. 5, serious days (DVI>10) like October 16th, 2015 can account for around 20% of total days and this proportion can be larger in summer. Therefore, it is necessary to improve the voltage regulation performance and mitigate excessive SVR tap operations in large PV power fluctuating days. Voltage regulation performance and the amount of SVR tap operations in one day with different DVIs are compared in Table II.

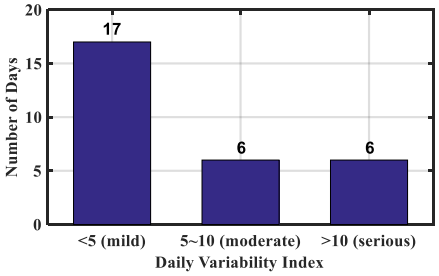

Fig. 5 DVI distribution of October.

TABLE I
THE PERCEPTIBILITY STANDARD [20]

Relative voltage variation thresholds	0.8%	1.0%	1.3%	1.5%
Maximum occurrences allowed per day	50	30	10	5

TABLE II
COMPARISONS OF VOLTAGE REGULATION PERFORMANCE AND AMOUNT OF SVR TAP CHANGES IN DAYS WITH DIFFERENT DVI VALUES

PV Power Profiles	ΔV>0.8%	ΔV>1.3%	Tap Changes
Oct 16th, DVI=11.3 (serious)	57	18	50
Oct 22th, DVI=7.7 (moderate)	17	6	36
Oct 11th, DVI=3.8 (mild)	10	2	10

III. PARAMETER RESELECTION FOR THE POWER FACTOR DROOP CURVE

The characteristics of voltage regulation from an SVR and the reactive power support are different. On the one hand, the SVR is designed to compensate slow changes in load and upstream voltage, but not to counter fast PV power fluctuations. If the reactive power support from PV inverters can effectively alleviate voltage variations caused by intermittent PV power generation, excessive SVR tap changes can be successfully reduced. On the other hand, although fast reactive power response is effective to mitigate PV power fluctuations, its voltage regulation ability is limited to the power factor range specified by the local utility. If the voltage profile drifts away too much from the pre-set operational range of PV inverters due to slow load variations, the reactive power support will not be as effective as designed. Therefore, for efficient utilization of limited reactive power capacity restricted by power factor, the reactive power support also needs the SVR to compensate slowly changing quantities (*e.g.* load, upstream voltage) in a distribution system. In this section, the following content on the way of achieving such coordination between upstream SVR and local reactive power support is organized as follows:

i) The voltage regulation from the SVR is introduced in Part A. Around the operational range provided by the SVR, an innovative method of using a voltage-PV generation curve is established to analyze the voltage response of PV power with a given power factor droop curve in Part B.

ii) Two PV power fluctuation characteristics can be abstracted from the statistics of PV power historical data in Part C, which will be used in the established optimization model in Part D.

iii) In Part D, based on the voltage-PV generation curve developed in Part B, power factor droop parameters (V_{low}, V_{m1}, V_{m2} and V_{high}) are optimally reselected according to the PV power fluctuation characteristics obtained in Part C.

A. Voltage Regulation from the SVR

As shown in Fig. 3, a 32-step SVR controlled by the Line Drop Compensation (LDC) rule is installed between node 4 and node 5 regulating the remote node voltage. No communication between SVR and the PV plant is needed. The simulation network setting are as follow: 1) the voltage of node 8 (campus load node with a PV plant connected) is regulated by the SVR; 2) the voltage target V_{target} of the SVR is set to be 0.99pu, with a dead band ΔV_{db} of ±0.01pu; 3) the time delay of SVR tap operations is set to be 2 minutes [21];

Before the beginning of analyzing the voltage regulation performance from reactive power support, the SVR tap is assumed to be already on a stable position.

B. Voltage Regulation from Reactive Power Support

If the SVR tap has already switched to a reasonable position to fit a certain load level and remain unchanged for a period of time, the voltage response of PV generation can be described by a voltage-PV generation curve, as shown in Fig. 6. This voltage-PV generation curve can be obtained from the power factor droop curve as in Fig. 1 with fixed load level and SVR tap position. Through this voltage-PV generation curve, PV generation is mapped to the voltage, and four inflection points on this curve are corresponding to the parameters (V_{low}, V_{m1}, V_{m2}, V_{high}) on the power factor droop curve respectively.

As a result, the voltage-PV generation curve in Fig. 6 can be defined by V_{low}, V_{m1}, V_{m2}, V_{high} that reveal the changing rule of the power factor with respect to voltage. Two dashed lines in Fig. 6 represent the limits of the power factor which has to be respected at all times.

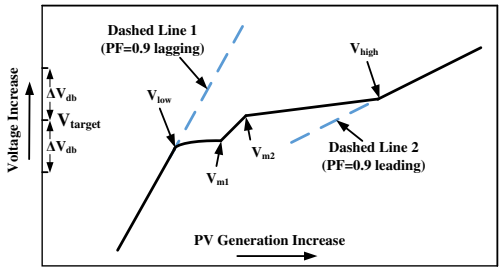

Fig. 6 Voltage-PV generation curve.

C. The Characteristics of PV Power Fluctuations

The relationship between PV generation value and the frequency of PV power fluctuation will be established in this section. Firstly, a synthetic PV power profile (Fig. 7) is used as a simple example to explain how to obtain such relationship.

As in Fig. 7 (a), PV power first increases from 0MW to 2MW, then reduces to 1MW before increases to 2MW again, and finally, it falls from 2MW to 0MW. Therefore, in this case, PV power is more likely to fluctuate in the range of [1MW, 2MW] (4 times) than in the range of [0MW, 1MW] (2 times). Correspondingly, the relationship between PV generation value and the frequency of PV power fluctuation can be developed as in Fig. 7 (b). An intuitive insight can be obtained from Fig. 7 (a) that more PV power plots are "overlapped" in the range from 1MW to 2MW (4 times) compared with that of the range from 0MW to 1MW (2 times).

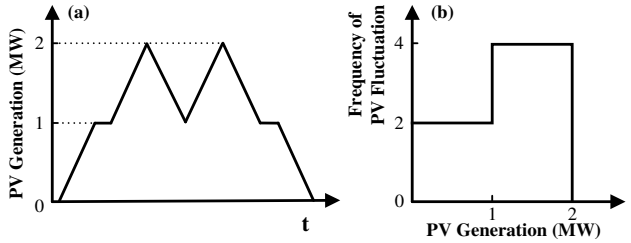

Fig. 7 PV generation profile (a) and the frequency of PV power fluctuation with PV generations (b).

Similar to Fig. 7 (b), Fig. 8 demonstrates the relationship between PV generation value and the normalized frequency of PV power fluctuation with real PV historical data, and a normal distribution curve is used to fit the original curve. As expected, the frequency of large power fluctuation is low when PV generation value approaches to zero or its maximum (rated) value.

There are two characteristics can be obtained from Fig. 8 that will be used in the latter optimization model:

Characteristic One: Large PV power fluctuations (e.g. PV power fluctuations larger than 0.4MW will cause significant voltage variations in the Gatton distribution system) almost only occur in the range from PV_{low} to PV_{high}. As in Fig. 8, PV_{low} and PV_{high} satisfy that the normalized frequency of large PV power fluctuation is lower than ε (a small positive value) if PV generation is lower (larger) than PV_{low} (PV_{high});

Characteristic Two: Large PV power fluctuations occur most frequently in the range [μ-σ, μ+σ]. μ and σ are expectation and standard deviation of the fitting normal distribution curve.

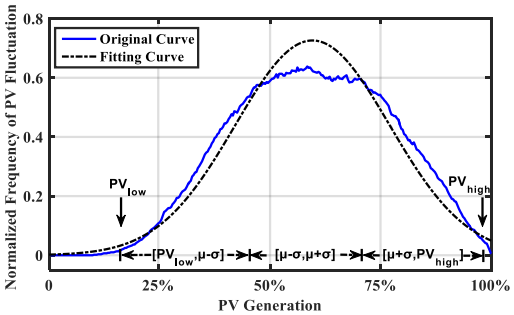

Fig. 8 Normalized frequency of PV power fluctuation with PV generations.

D. Optimization Model for Parameter Reselection

In this part, ***Characteristic One*** and ***Characteristic Two*** obtained in Part C are used to optimally reselect the four parameters (V_{low}, V_{m1}, V_{m2}, V_{high}) for the power factor droop curve.

1) Utilization of Characteristic One

As large PV power fluctuations almost only occur in the range from PV_{low} to PV_{high}, a straightforward idea to alleviate significant voltage variations caused by PV power fluctuations is trying to reduce the voltage deviation $\Delta V'$ between these two extreme PV generation scenarios, namely

$$\Delta V' = V_{PVhigh} - V_{PVlow} \tag{3}$$

where V_{PVlow} and V_{PVhigh} represent the node voltages when PV generation is equal to PV_{low} and PV_{high} respectively.

Fig. 6 shows the voltage response of PV generation with a given power factor droop curve, and it is redrawn as in Fig. 9. In this figure, the voltage-PV generation curve first follows the Dashed Line 1 (PF=0.9 lagging) when PV generation is low. Then this curve leaves the Dashed Line 1 after the first inflection point V_{low} as PV generation increases. Finally, this curve overlaps with the Dashed Line 2 (PF=0.9 leading) after the last inflection point V_{high}. Therefore, the positions of first and last inflection points of the voltage-PV generation curve are determined by the setting of V_{low} and V_{high} respectively.

In Fig. 9, **Intersection 1** is defined as the crossing point of the line $PV = PV_{low}$ and the Dashed Line 1, so is **Intersection 2** of the line $PV = PV_{high}$ and the Dashed Line 2. If the first inflection point V_{low} and the last inflection point V_{high} are situated within these two intersection points, the voltage deviation $\Delta V'$ due to PV power drop from PV_{high} to PV_{low} will be almost constant ($\Delta V' = V_{Intersection2} - V_{Intersection1}$ in Fig. 9). Conversely, if the first inflection point (V_{low2}) is set to be lower than the **Intersection 1**, this voltage deviation will become larger ($\Delta V'' = V_{Intersection2} - V_{PV_{low}}$). Therefore, for obtaining a low voltage deviation $\Delta V'$ between the two extreme PV generation scenarios, V_{low} and V_{high} should satisfy (4).

$$V_{low} \geq Intersection\ 1$$
$$V_{high} \leq Intersection\ 2 \quad (4)$$

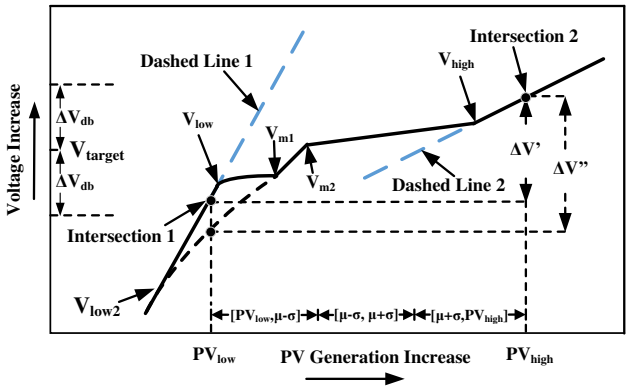

Fig. 9 Voltage deviation between two intersections.

2) Utilization of Characteristic Two

The voltage-PV generation curve in Fig. 9 reflects the voltage response with respect to PV generation. Consequently, different curve slopes (voltage vs PV generation) mean that for the same change of PV generation, different voltage variations will occur due to different reactive power supported by PV inverters.

The voltage deviation between two extreme PV generation scenarios (PV_{low} and PV_{high}) will be constant, as long as constraints in (4) are satisfied. Therefore, a lower slope on one part of the voltage-PV generation curve will cause a higher slope on another part of this curve. In other words, slopes on different parts of the curve have a competing relationship between each other. Therefore, the strategy is to assign a low slope to the PV generation range [μ-σ, μ+σ] where large PV power fluctuations most likely to occur. Consequently, the objective function can be written as

$$Minimize\ L \quad (5)$$

where L is the maximum curve slope in the range of [μ-σ, μ+σ], and slopes between any two points on the voltage-PV generation curve within this range cannot be larger than L. As slope varies on the whole voltage-PV generation curve, in order to simplify calculation, the voltage-PV generation curve within the range of [μ-σ, μ+σ] is divided evenly into n segments according to PV generation. And average slope of each segment i is restrained by L, as

$$\frac{V_{pv(i+1)}-V_{pv(i)}}{pv(i+1)-pv(i)} \leq L \quad i = 1,2,\dots,n \quad (6)$$

where $V_{pv(i)}$ represents the node voltage when PV generation is equal to $pv(i)$, and $pv(1)=\mu-\sigma$, $pv(n+1)=\mu+\sigma$, $pv(i+1)=pv(i)+2\sigma/n$. $pv(i)$ can be calculated in advance according to μ, σ and n. The relationship between $V_{pv(i)}$ and $pv(i)$ is given as the constraints in (7) and (8),

$$f_1\left(pv(i), PF_{pv(i)}, V_{pv(i)}\right) = 0 \quad (7)$$

$$PF_{pv(i)} = f_2(V_{pv(i)}) \quad (8)$$

where f_1 represents the power flow equation set and f_2 represents the relationship between the power factor $PF_{pv(i)}$ of PV inverters and the voltage $V_{pv(i)}$ of the PV connection point. It should be noticed that (8) is the piecewise power factor droop curve which is characterized by parameters V_{low}, V_{m1}, V_{m2}, V_{high}, as shown in Fig. 1.

Furthermore, the competing relationship for different parts of the curve mentioned before can be balanced through limiting the curve slope in the range of [PV_{low}, μ-σ] as in (9). The parameter c is the predetermined upper limit of curve slope. The selection and comparison of different parameter c will be discussed later in case studies.

$$\frac{V_{pv(1)}-V_{PV_{low}}}{pv(1)-PV_{low}} \leq c \quad (9)$$

IV. The Voltage-PV Generation Curve with Variable Load and SVR Tap Operations

A. Interaction between SVR and Variable Load

In this section, the effectiveness of the predefined voltage-PV generation curve will be demonstrated with variable load. The offsetting interaction between SVR tap operation and load variation will be discussed as follow, which can limit the movement of the predefined voltage-PV generation curve caused by load variation to a low level.

Fig. 10 demonstrates that the position of the voltage-PV generation curve will be changed with different load or SVR tap position. As shown in Fig. 10, the curve is moved towards left when load decreases or SVR tap position is stepped up, while the curve is moved towards right when load increases or SVR tap position is stepped down.

Compared with fast fluctuating PV power, load variation is much slower and can be regarded as constant in a short period. As a result, during this short period, the trajectory of (PV Generation, Voltage) Node will approximately follow the voltage-PV generation curve. However, accumulated load variation will cause movement of the voltage-PV generation curve as in Fig. 10, until a SVR tap operation is triggered to offset this impact. Therefore, the movement of the predesigned voltage-PV generation curve will always be limited to a low level, due to the offsetting interaction between SVR tap operation and load variation.

Fig. 11 demonstrates the load and PV data recorded in Gatton campus for one day as an example. As in Fig. 11, the load creeps from 1.26MW at early morning (3:30) to 2.79MW at noon (14:00) with an increment of 120%. Using these real data, Fig. 12 shows the distribution of (PV Generation, Voltage) Nodes from 9:00 to 14:00 obtained from power flow calculations with a resolution of 1 minute. During this period, the load creeps from 2MW at 9:00 to 2.79MW at 14:00 with an increment of 40%, and SVR changes its tap positions for 4 times. (PV Generation, Voltage) Nodes are denoted as pentagrams, triangles, circles, asterisks and dots respectively corresponding to the variation of SVR tap positions. It can be seen all nodes gather around the predefined voltage-PV generation curve, especially in the range of [μ-σ, μ+σ], where large PV power fluctuations occur most frequently. Therefore, it is reasonable to decouple the voltage regulation analysis of reactive power support from the load variation (can be offset

by SVR), and the effectiveness of proposed method can be guaranteed.

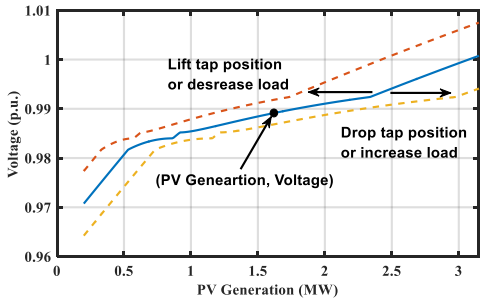

Fig. 10 Opposite impact from variable load and SVR tap position

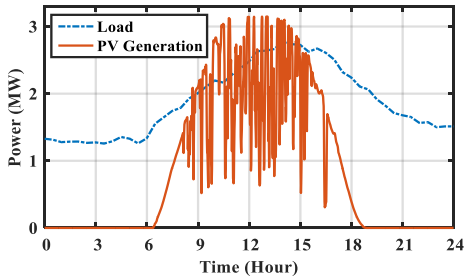

Fig.11 Load and PV power profile of October 16th, 2015.

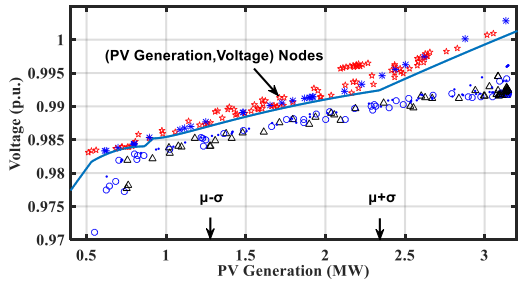

Fig.12 Distribution of (PV Generation, Voltage) Nodes with different SVR tap positions

B. Load Level and SVR Tap Position for the Voltage-PV Generation Curve

For the Gatton distribution system, the correspondence between SVR tap position and load level is already known. Therefore, using existing data, the voltage-PV generation curve will exactly lie within the SVR allowable voltage range such as [0.98pu,1.0pu]. While, in order to generalize our method, we also discuss how to determine the voltage-PV generation curve with an allowable voltage range of SVR when the correspondence between SVR tap position and load level is unknown.

A voltage-PV generation curve can provide a mapping from a PV generation range $[PV_{low}, PV_{high}]$ to a voltage variation range $[V_{low}, V_{high}]$ as in Fig. 13 (solid line). Namely, PV_{low} and V_{low} are the x-axis and y-axis values of **Intersection 1**; PV_{high} and V_{high} are the x-axis and y-axis values of **Intersection 2**. As a result, voltage will mainly fluctuate within the range $[V_{low}, V_{high}]$ due to PV power variations. This voltage variation range $[V_{low}, V_{high}]$ should be consistent with the allowable voltage range of SVR, namely $[V_{target} - \Delta V_{db}, V_{target} + \Delta V_{db}]$. Otherwise, for example, if V_{high} is larger than $V_{target} + \Delta V_{db}$, SVR tap operation will be frequently triggered by PV power fluctuations. As a result, excessive SVR tap operations can be expected.

The position of a voltage-PV generation curve can be adjusted by applying different load and SVR tap position, and $[V_{low}, V_{high}]$ will moves accordingly. As in Fig. 13, two voltage-PV generation curves with same parameters (V_{low}, V_{m1}, V_{m2}, V_{high}) locate in different positions (with different load or SVR tap position). Compared with $[V_{low}, V_{high}]$, $[V'_{low}, V'_{high}]$ has a downward movement.

Therefore, before solving the optimization problem established in Section III Part D, suitable load and SVR tap position should be applied on the voltage-PV generation curve to make $[V_{low}, V_{high}]$ consistent with the allowable voltage range of SVR. Due to the offsetting interaction between SVR and load, the suitable SVR tap position and load level for the voltage-PV generation curve are not unique.

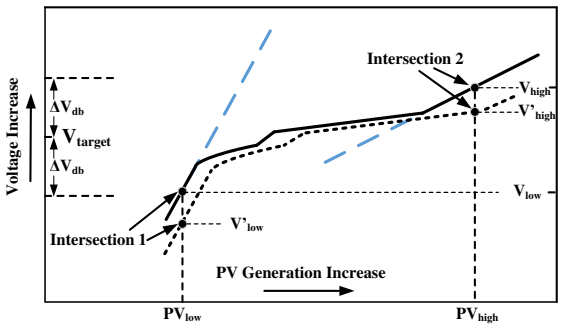

Fig. 13 Mapping from PV generation range to voltage range

V. Summary

According to the proposed method, the SVR is used to compensate slowly changing quantities, so that the movement of the predefined voltage-PV generation curve can be limited to a low level. While, the reactive power support is designed to counter fast fluctuating PV power. This is how the coordination is designed, and it mainly reflects in two aspects:

1) On one hand, the limited reactive power support restricted by allowable power factor range is used to mitigate the voltage fluctuations caused by large PV power variations. As long as the voltage fluctuations become insignificant, system voltage can be successfully controlled by SVR with a few tap operations. Otherwise, SVR tap operations may be frequently triggered by large voltage fluctuations. As a result, excessive SVR tap operations may occur.

2) On the other hand, the voltage regulation performance of the reactive power support from the PV plant relies on the existence of SVR. The voltage-PV generation curve will change its position due to load variation, as in Fig. 10. However, considering the offsetting interaction between SVR and load, large load deviations during a day can always be compensated by SVR tap operations. As a result, the mismatch of the relationship between voltage and PV generation established by the predesigned voltage-PV generation curve can always be limited to a low level.

Simulations in the case studies show excessive SVR tap operations can be mitigated after the application of the optimal parameters, which verifies the first aspect of the coordination.

While in Fig. 12, all the (PV Generation, Voltage) Nodes gather around the predesigned voltage-PV generation curve, which verifies the second aspect of the coordination.

The proposed method in this paper can be generalized as three steps (Fig. 14):

i) Obtain ***Characteristic One*** and ***Characteristic Two*** from statistics of PV power historical data.

ii) Select suitable load level and SVR tap position for the voltage-PV generation curve, so that $[V_{low}, V_{high}]$ can be consistent with $[V_{target} - \Delta V_{db}, V_{target} + \Delta V_{db}]$.

iii) On the basis of the voltage-PV generation curve, optimally reselect the power factor droop parameters according to the established optimization model (4)~(9).

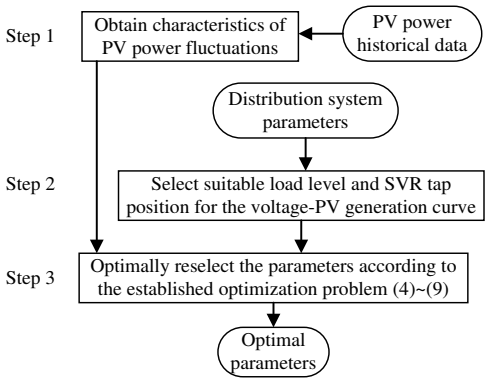

Fig. 14 Flow chart for optimally reselecting parameters.

VI. Multiple PV Plants

In order to apply the proposed method in a more general distribution system with multiple PV plants, another sub feeder in Fig. 2 regulated by SVR B is considered as in Fig. 15. As shown in this figure, PV plants will be connected at node 6, 8 and 13.

Since the power factor droop curve is one kinds of local voltage dependent reactive power support methods, hunting behavior may occur between different PV inverters [22]. In order to solve this issue, the reactive power $Q_i(t)$ generated by the PV plant connected at node i at time instant t should be modified as [22]

$$Q_i(t) = \left(1 - \frac{\Delta T}{\tau}\right) Q_i(t - \Delta T) + \frac{\Delta T}{\tau} q_i[V_i(t)] \tag{10}$$

where $V_i(t)$ represents the measured local voltage at node i at time instant t; $q_i[V_i(t)]$ represents the reactive power required according to the predefined power factor droop curve; Sampling time ΔT is set to be 1s, while time constant τ is 10s. The stability of (10) has already been proved in [22].

A. PV Plants Connected at Node 8 and 13

In this section, two PV plants are connected at different sub feeders (node 8 and node 13). If voltage of node 13 is regulated by SVR B, the proposed method also can be used to optimally select power factor droop parameters for the PV plant at node 13. Since reactive power support cannot totally compensate PV power variations, mild upstream voltage fluctuations can be caused by the additional PV plant. However, similar to load variations, such mild upstream voltage fluctuations also can be offset by the downstream SVR. In such situations, power factor droop parameters can be optimized separately for these two PV plants.

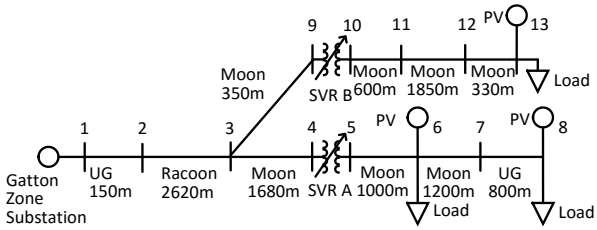

Fig. 15 The Gatton distribution system with multiple PV plants.

B. PV Plants Connected at Node 6 and 8

In this section, two PV plants are installed downstream of SVR A (node 6 and node 8), and two loads are connected at node 6 and 8 as in Fig. 15. The multiple PV plants scenario can be firstly converted to one equivalent PV plant scenario. Then, the proposed method can be used to optimally select power factor droop parameters for the equivalent PV plant. The procedure to obtain the equivalent virtual PV plant can be divided into four steps.

1) Select the Position of the Equivalent PV Plant

The position of the equivalent PV plant can be determined considering the line impedance and PV capacities. This position is represented by the value of line impedance as

$$z_{6\_r} = z_{6\_8} \frac{P_{pv8}}{P_{pv6} + P_{pv8}} \tag{11}$$

where z_{6_r} and z_{6_8} represent line impedance from node 6 to the position of the equivalent PV plant at point r and from node 6 to node 8 respectively. P_{pv6} and P_{pv8} are capacities of PV plants at node 6 and 8 respectively.

2) Calculate Equivalent PV Capacities and Loads at Point r

The capacity of the equivalent PV plant P'_{pvr} can be obtained through converting PV capacities to point r as

$$P'_{pvr} = P_{pv8} + \frac{r_{1\_6}}{r_{1\_r}} P_{pv6} \tag{12}$$

where r_{1_6} and r_{1_r} are line resistance from node 1 to 6 and from node 1 to point r respectively. Similarly, equivalent load P'_{lr} at point r can be obtained as

$$P'_{lr} = P_{l8} + \frac{r_{1\_6}}{r_{1\_r}} P_{l6} \tag{13}$$

where P_{l6} and P_{l8} represent peak load at node 6 and node 8 respectively. As in (12) and (13), all parameters are converted to point r with the principle of keeping the voltage at point r constant.

3) Set LDC Impedance

In this paper, the upstream SVR A senses both active and reactive current as well as the local voltage of node 5 to estimate remote node voltage with an equivalent impedance. The equivalent LDC impedance z_e can be determined as

$$z_e = \alpha z_{pv} + (1 - \alpha) z_l \tag{14}$$

where z_{pv} and z_l as expressed in (15) and (16) represent the equivalent impedances only considering the effect of PV

plants and loads respectively. Parameter α is used to balance the effect of PV plants and loads in the decision of the LDC impedance z_e. The value of α can be set by distribution system operators.

The equivalent PV capacity at point r is P'_{pvr}, while SVR senses PV power with a value of $P_{pv6} + P_{pv8}$ at node 5 when no load is connected at node 6 and 8. Therefore, the equivalent impedance only considering the effect of PV plants can be obtained as

$$z_{pv} = z_{5\_r} \frac{P'_{pvr}}{P_{pv6}+P_{pv8}} \tag{15}$$

where z_{5_r} represents impedance from node 5 to point r. Similarly, the equivalent impedances only considering the effect of loads can be obtained as

$$z_l = z_{5\_r} \frac{P'_{lr}}{P_{l6}+P_{l8}} \tag{16}$$

4) Equivalent PV Statistical Parameters

Without loss of generality, the PV plants at node 6 and 8 are assumed to have different statistics of PV power fluctuation behaviors. In this situation, the equivalent parameters PV'_{low}, PV'_{high}, μ', σ' for the equivalent PV plant at point r can be obtained as formulated in (17)-(20) below. The basic principle for equivalence is the same as that of (12) and (13). The only difference is that PV'_{low} is chosen to be the lowest value between the PV plants in order to make sure the selection of an appropriate low point of PV power.

$$PV'_{low} = min(PV_{low,8}, \frac{r_{1\_6}}{r_{1\_r}} PV_{low,6}) \tag{17}$$

$$PV'_{high} = PV_{high,8} + \frac{r_{1\_6}}{r_{1\_r}} PV_{high,6} \tag{18}$$

$$\mu' = \mu_8 + \frac{r_{1\_6}}{r_{1\_r}} \mu_6 \tag{19}$$

$$\sigma' = \sigma_8 + \frac{r_{1\_6}}{r_{1\_r}} \sigma_6 \tag{20}$$

where $PV_{low,6}$, $PV_{high,6}$, μ_6, σ_6 can be obtained from the statistics of PV historical data at node 6 (refer to Fig. 8); $PV_{low,8}$, $PV_{high,8}$, μ_8, σ_8 can be obtained from the statistics of PV historical data at node 8.

The optimal parameters (V_{low}, V_{m1}, V_{m2}, V_{high}) of the power factor droop curve are designed according to the statistics of historical PV power fluctuation behaviour of the equivalent PV plant. Then, the same parameters from the equivalent PV system are assigned to both the PV plants at nodes 6 and 8. The reasons are as follows:

(1) Since SVR can only target at one point of the feeder for voltage regulation, an equivalent PV plant is required for the proposed coordination design. Therefore, the control parameters of the two PV plants cannot be individually designed when considering coordination.

(2) Voltage variations at node 6 (or node 8) are influenced by PV power fluctuations from both PV plants, instead of the individual PV system at each node. Such a combined effect is aggregated into the equivalent PV plant, and the resultant optimal parameters are exactly designed for this aggregated PV power fluctuating effect. Therefore, optimal parameters obtained from the equivalent PV plant are effective for both PV plants at nodes 6 and 8, even when their power outputs vary in the same manner (the worst case scenario). Hence, using the same parameters obtained from the equivalent PV plant for both PV systems at nodes 6 and 8 is a reasonable and effective approximation. If the two PV plants have totally different fluctuation behaviors, their total effect cannot exceed the worst case which have already been considered. Therefore, the designed control parameters should be adequate for voltage regulation.

VII. Algorithm and Simulation

A. Solving Optimization Problem

The optimization model has been developed with objective function (5), linear inequality constraints (4), (6) and (9), nonlinear equality constraints (7) and (8) in Section III. In this paper, the particle swarm optimization (PSO) algorithm is selected to solve the formulated optimization problem. The optimization variables are four parameters of the power factor droop control curve, namely V_{low}, V_{m1}, V_{m2} and V_{high} (V_{low}<V_{m1}<V_{m2}<V_{high}). This proposed optimization model is for the planning and designing stage, and parameters will not vary with the time during operation once they are determined from the optimization. Hence, computation time is not a major issue. The resolution of PV data used in our simulations is one minute. The time needed to solve this optimization problem is less than 3 minutes.

B. Checking the Performance

A quasi-static time-series power flow program is developed to test the voltage regulation performance and count the amount of SVR tap operations during a day. Real data of load demand and PV generation are used in all simulations. Since the response of reactive power support from PV inverters is much faster than the tap operation of SVR, the voltage regulation from PV inverters is regarded to be finished instantaneously in this paper. Therefore, in each time instant, firstly the power flow regulated only by PV inverters is calculated. Then the SVR tap position changing conditions (*i.e.* time delay, overvoltage, low voltage) will be checked to determine whether an SVR tap operation is required. If SVR tap position does not change, the power flow of the next time instant will be calculated and the time delay of the SVR will be updated. Otherwise, power flow regulated only by PV inverters should be calculated again with updated SVR tap position, and the SVR time delay will be initialized to zero.

VIII. Case Study

In this section, distribution system as in Fig. 3 is used for one PV plant simulations in Part A to C. Real PV data recorded in the 3.15MW PV plant at Gatton campus are used in simulations. While distribution system as in Fig. 15 is used for simulations of multiple PV plants in Part D and E. SVR A and B sense both real and reactive current as well as the local voltage at their secondary side to estimate remote node

voltage. Except for specific indication, LDC impedance of SVR A is modelled as R+jX=0.694+j0.630Ω;

A. The Impact of Constraints on V_{low} and V_{high}

Seven case studies (Case 1 to Case 7) are compared in Table III. The recorded PV generation and load data of October 16th, 2015 as in Fig. 11 are used in simulations. The voltage regulation performance with original parameters (Case 2) is the worst among all seven simulation results. The number of relative voltage variations larger than 0.8% and 1.3% are 57 and 18 respectively, which violate the perceptibility standard given in Table I. In addition, the amount of SVR tap changes is as high as 50 times, which implies the SVR tap operations are frequently triggered by fast fluctuating PV power. This is not preferred as a shorter life span and higher maintenance cost of the SVR can be expected.

Fig. 16 compares two voltage-PV generation curves obtained from the current setting (Case 2) and the optimization (Case 4) respectively. As shown in Fig. 16, the parameters of current setting (Case 2) do not satisfy with the constraints in (4) (V_{low} is too low to be displayed in this figure). As a result, this voltage-PV generation curve will have a larger voltage deviation between two extreme PV generation scenarios ($PV_{low} = 0.5MW$ and $PV_{high} = 3.15MW$). Therefore, compared with Case 4, larger voltage fluctuations can be expected in Case 2. In addition, due to bad voltage regulation performance of reactive power support in Case 2, SVR tap operations are more likely to be triggered.

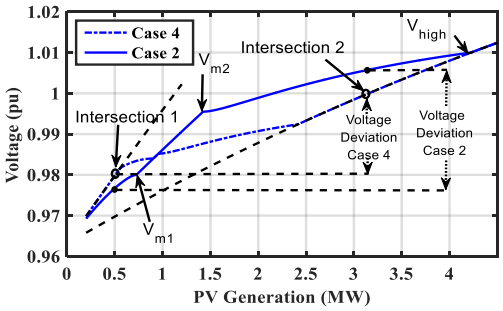

Fig. 16 Voltage-PV generation curves comparison (Case 2 vs Case 4).

In Case 7, four power factor droop parameters are evenly distributed among the SVR allowable voltage range [0.98,1.0], namely, V_{low}=0.98, V_{m1}=0.986, V_{m2}=0.994, V_{high}=1.0. Compared with original parameters, the evenly distributed parameters have better performance both in voltage regulation and the amount of SVR tap operations. However, the evenly distributed parameters cannot work as well as optimal parameters in voltage regulation performance. This is because the evenly distributed parameters only reduce the voltage deviation between two extreme PV generation scenarios (PV_{low} and PV_{high}), but do not assign a lower slope (voltage vs PV generation) to the range where large PV power fluctuations most likely to occur for the voltage-PV generation curve.

B. The Impact of Different Parameter c

Different selections of parameter c in (9) are compared and discussed in this section.

1) Parameter c with Relative Large Value

When parameter c in (9) is set to be a relatively large value (*e.g.* 0.03 as in Case 3), it means the constraint in (9) is too loose. As a result, a lower value of the objective function in (5) can be obtained. In other words, on the voltage-PV generation curve, a lower slope can be achieved corresponding to the PV generation range of [μ-σ, μ+σ] (μ=1.88MW, σ=0.55MW), at a cost of increasing the curve slope corresponding to the PV generation range of [0.5MW, μ-σ], as shown in Fig. 17. In this figure, the slope of the voltage-PV generation curve (Case 3) in the range of [μ-σ, μ+σ] is almost equal to zero. However, its slope in the range of [0.5MW, μ-σ] becomes steeper compared with that of the curve of Case 4. Consequently, larger voltage fluctuations can be expected when PV power fluctuates in the range of [0.5MW, μ-σ].

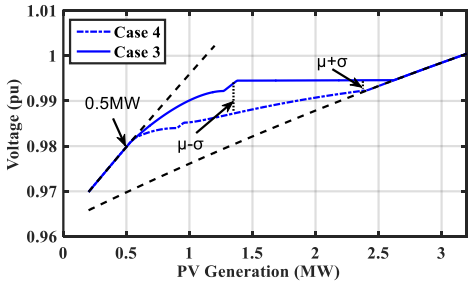

Fig. 17 Voltage-PV generation curves comparison (Case 3 vs Case 4).

2) Parameter c with Relative Small Value

If parameter c in (9) is set to be a relatively small value (*e.g.* 0.004 as in Case 5), it means the constraint in (9) is too strict. Hence, the slope of the curve in the range of [μ-σ, μ+σ] (namely objective function) has to be sacrificed in order to avoid violating the constraint in (9). As shown in Fig. 18, compared with Case 4, the curve slope of Case 5 (c=0.004) is steeper in the range of [μ-σ, μ+σ]. Consequently, larger voltage fluctuations can be expected when PV power fluctuates in the range of [μ-σ, μ+σ].

TABLE III
VOLTAGE REGULATION PERFORMANCE WITH DIFFERENT PARAMETERS

	Parameters	ΔV>0.8%	ΔV>1.3%	Tap Changes	How to Obtain
Case 1	No PV Plant Connected	1	1	8	Not Applicable
Case 2	V_{low}=0.960, V_{m1}=0.980, V_{m2}=0.996, V_{high}=1.010	57	18	50	Current Setting
Case 3	V_{low}=0.981, V_{m1}=0.992, V_{m2}=0.994, V_{high}=0.995	11	2	6	Optimization (c=0.03)
Case 4	V_{low}=0.982, V_{m1}=0.984, V_{m2}=0.985, V_{high}=0.992	4	1	6	Optimization (c=0.008)
Case 5	V_{low}=0.981, V_{m1}=0.982, V_{m2}=0.983, V_{high}=0.984	9	1	6	Optimization (c=0.004)
Case 6	V_{low}=0.983, V_{m1}=0.984, V_{m2}=0.985, V_{high}=0.996	6	2	6	Optimization (even slope)
Case 7	V_{low}=0.98, V_{m1}=0.986, V_{m2}=0.994, V_{high}=1.0	24	1	6	Evenly Distributed Parameters

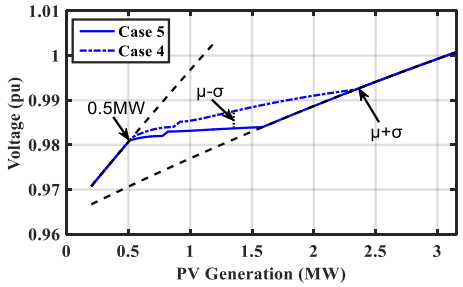

Fig. 18 Voltage-PV generation curves comparison (Case 4 vs Case 5).

3) Discussion

Comparing voltage regulation results (ΔV>0.8%, ΔV>1.3%) from Case 2 to Case 5 in Table III, the differences between Case 2 and Cases 3~5 are definitely larger than the differences among Cases 3~5 themselves. It reveals that the voltage regulation performance is more sensitive to the constraints in (4) than the different selection of parameter c. Therefore, compared with the method proposed in Section III Part D, a simplified optimization model can be established by eliminating (9) and extending the applicable range of (6) from [μ-σ, μ+σ] to [PV_{low}, PV_{high}], which implies $pv(1)$=0.5MW, $pv(n+1)$=3.15MW, $pv(i+1)=pv(i)+2.65\text{MW}/n$ for (6). This means the simplification tries to make the curve slope as even as possible in the range of [0.5MW, 3.15MW] in Case 6.

Curves of Case 4 and Case 6 are compared in Fig. 19. Case 4 emphasizes to reduce the curve slope corresponding to the PV generation range of [μ-σ, μ+σ], and at the same time the slope in the range of [0.5MW, μ-σ] is limited by the constraint in (9) with a suitable value of parameter c. While Case 6 tries to make the curve slope as even as possible between two extreme PV generation scenarios (PV_{low} and PV_{high}).

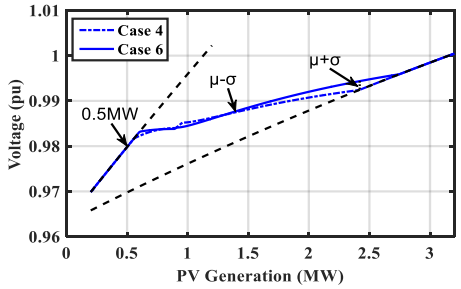

Fig. 19 Voltage-PV generation curves comparison (Case 4 vs Case 6).

Finally, it should be noticed that the amounts of SVR tap operations during a day in Case 3 to Case 6 are similar to that of Case 1 when no PV plant is connected. It implies that the SVR is mainly used to compensate slowly changing quantities (*e.g.* load) rather than PV power fluctuations in the proposed method, as long as reactive power support can successfully mitigate voltage fluctuations.

C. Voltage Fluctuations from Upstream

Except for the variations of load and PV generation, upstream voltage fluctuations will also influence the voltage regulation in distribution systems. However, the same as the load, the upstream voltage is mostly a slowly changing quantity, as shown in Fig. 20. Hence, the PV power remains the dominant fluctuating quality in a short timescale, and the SVR tap operations can offset large variations of slowly changing quantities (load and upstream voltage) in a long timescale. Consequently, the method proposed in this paper remains effective. As shown in Table IV, the upstream voltage has little influence on voltage regulation performance. However, more SVR tap operations are required to compensate the voltage fluctuations from upstream.

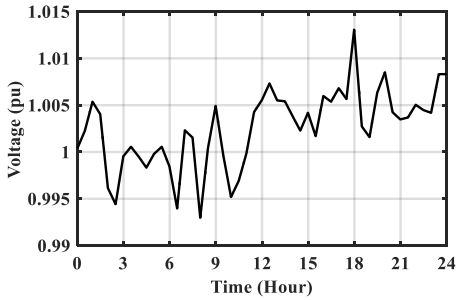

Fig. 20 Upstream voltage fluctuations.

TABLE IV
VOLTAGE FLUCTUATIONS FROM UPSTREAM

Parameters	ΔV>0.8%	ΔV>1.3%	Tap Changes	Upstream Voltage
Original (Case 2)	57	18	50	Constant (1.01)
	60	19	56	Real Voltage Data
Optimal (Case 4)	4	1	6	Constant (1.01)
	5	1	8	Real Voltage Data

D. Two PV Plants Connected at Node 8 and 13

On the basis of previous simulations, another PV plant with capacity of 1MWp is connected at node 13. The same as SVR A, SVR B regulates the voltage of node 13 within [0.98pu,1.0pu]. The LDC impedance of SVR B is set to be R+jX=0.779+j0.700Ω.

Voltage regulation performance with optimal and original parameters are compared in Table V. Compared with original parameters, the optimal parameters can improve voltage regulation performance and mitigate excessive SVR tap operations.

TABLE V
TWO PV PLANTS CONNECTED AT NODE 8 AND NODE 13

	ΔV>0.8%	ΔV>1.3%	Tap	V_{low}, V_{m1}, V_{m2}, V_{high}
Node 8	69	27	70	0.960, 0.980, 0.996, 1.010 (Original)
	5	2	10	0.982, 0.984, 0.985, 0.992 (Optimal)
Node 13	34	6	28	0.960, 0.980, 0.996, 1.010 (Original)
	4	0	8	0.986, 0.987, 0.988, 0.992 (Optimal)

For the PV plant at node 8, the interference caused by the PV plant at node 13 mainly lies in the variation of upstream voltage, and vice versa. Therefore, the analysis in this section is similar to the analysis in Section VIII Part C (the impact from upstream voltage fluctuations is discussed). The integration of the second PV plant can increase the upstream voltage fluctuations. As a result, compare with the values in the grey area in Table IV, more SVR tap operations are required to offset the upstream voltage fluctuations as in Table V. At the same time, the voltage fluctuation extent at node 8 remains insignificant.

E. Two PV Plants Connected at Node 6 and 8

In this section, two PV plants with capacities of 1.5MWp and 1.65MWp (3.15MWp in total) are connected at node 6 and node 8 respectively, as shown in Fig. 15. In addition, the variable load as in Fig. 11 which was connected at node 8 are proportionally assigned to node 6 and 8 with percentages of 30% and 70% respectively.

1) LDC Voltage Control with Distributed Loads

According to the method proposed in Section VI Part B, the position of the equivalent PV plant is selected at 1.77km downstream of the SVR A. The equivalent LDC impedance z_e of SVR A is set to be R+jX=0.478+j0.427Ω.

Fig. 21 compares the voltage estimated by LDC scheme and the voltage obtained by power flow at point r when optimal parameters are applied. These two voltage profiles are almost overlapped. Therefore, the LDC voltage regulation scheme remain effective with distributed loads and PV plants as long as its equivalent LDC impedance can be reasonably set.

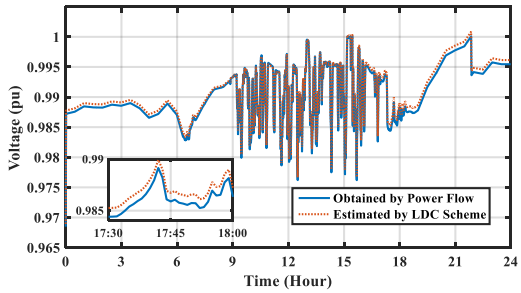

Fig. 21 LDC estimated voltage and voltage obtained from power flow

2) Voltage Regulation Performance and SVR Tap Operations

The voltage regulation performance and the volume of SVR tap operations are compared in Table VI with original and optimal parameters. As in this table, the proposed method remains effective with multiple loads and PV plants. Compared with original parameters, optimal parameters can always have better voltage regulation performance and less SVR tap operations.

TABLE VI
TWO PV PLANT CONNECTED AT NODE 6 AND NODE 8

	ΔV>0.8%	ΔV>1.3%	Tap	V_{low}, V_{m1}, V_{m2}, V_{high}
Node 6	44	12	26	0.960, 0.980, 0.996, 1.010 (Original)
	2	1	4	0.981, 0.982, 0.983, 0.994 (Optimal)
Node 8	58	14	26	0.960, 0.980, 0.996, 1.010 (Original)
	3	1	4	0.981, 0.982, 0.983, 0.994 (Optimal)

3) Different PV Power Profiles at Node 6 and 8

Two different PV power profiles with significant fluctuations recorded on Oct 18th and Oct 20th in the 3.15MWp Gatton PV plant are shown in Fig. 22. In this section, the recorded data will be proportionally scaled down according to the nominal capacities of PV plants at nodes 6 and 8. This is to mimic the situation with different PV power fluctuations at nodes 6 and 8.

The simulation results are shown in Table VII. The scaled PV data recorded on Oct 18th and 20th are allocated to the PV plants at nodes 6 and 8 respectively in Case A. While, for Cases B and C, PV power fluctuations at nodes 6 and 8 are assumed to be the same. Compared with Case A, slightly more voltage fluctuations can be observed in Cases B and C. This is due to the fact that with PV generation at nodes 6 and 8 swinging together in Cases B and C, significant overall PV power fluctuations are more likely to occur in Case B and C than in Case A. In summary, with optimal parameters, voltage fluctuations are insignificant in Cases B and C, and consequently it is not a concern for Case A either.

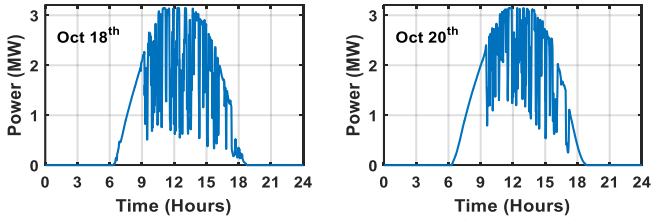

Fig. 22 Different PV power profiles recorded at Oct 18th and Oct 20th

TABLE VII
COMPARISON OF VOLTAGE REGULATION PERFORMANCE

		ΔV>0.8%	ΔV>1.3%	PV power Profiles
Case A	Node 6	1	1	Nodes 6 and 8 use scaled PV data recorded at Oct 18th and 20th respectively
	Node 8	2	1	
Case B	Node 6	3	1	Both nodes 6 and 8 use scaled PV data recorded at Oct 20th
	Node 8	3	1	
Case C	Node 6	5	2	Both nodes 6 and 8 use scaled PV data recorded at Oct 18th
	Node 8	11	2	

IX. CONCLUSION

For achieving better voltage regulation performance and mitigating excessive SVR tap changes, an innovative method of using the proposed voltage-PV generation curve is developed in this paper. Under such development, the reactive power support can be well coordinated with existing SVR in a weak distribution system. Such coordination can be obtained through optimally reselecting power factor droop parameters applied on PV inverters. With optimal parameter-fitted reactive power support, the SVR will mainly deal with slowly changing quantities (*e.g.* load and upstream voltage) as it is originally designed. On the other hand, limited reactive power capacity can be efficiently utilized to counter PV power fluctuations around the operational range provided by the SVR.

As demonstrated in case studies, the proposed method can successfully mitigate serious voltage variations and excessive SVR tap operations in large PV power fluctuating days. The proposed method also can be extended to the multiple PV plants scenario. Future PV integration projects in the fringe of the grid can benefit from the research methods developed in this paper.

X. ACKNOWLEDGMENT

This work was performed in part or in full using equipment and infrastructure funded by the Australian Federal Government's Department of Education AGL Solar PV Education Investment Fund Research Infrastructure Project. The University of Queensland is the Lead Research Organization in partnership with AGL, First Solar, and the

University of New South Wales.

XI. References

[1] M. Nijhuis, M. Gibescu, and B. Rawn, "Prediction of power fluctuation classes for photovoltaic installations and potential benefits of dynamic reserve allocation," *IET Renewable Power Generation,* vol. 8, pp. 314-323, 2014.

[2] R. F. Yan and T. K. Saha, "Investigation of Voltage Stability for Residential Customers Due to High Photovoltaic Penetrations," *IEEE Transactions on Power Systems,* vol. 27, pp. 651-662, May 2012.

[3] M. I. Hossain, T. K. Saha, and R. Yan, "Investigation of the interaction between step voltage regulators and large-scale photovoltaic systems regarding voltage regulation and unbalance," *IET Renewable Power Generation,* vol. 10, pp. 299-309, 2016.

[4] S. Deshmukh, B. Natarajan, and A. Pahwa, "Voltage/VAR Control in Distribution Networks via Reactive Power Injection Through Distributed Generators," *IEEE Transactions on Smart Grid,* vol. 3, pp. 1226-1234, Sep 2012.

[5] Z. Y. Wang, H. Chen, J. H. Wang, and M. Begovic, "Inverter-Less Hybrid Voltage/Var Control for Distribution Circuits With Photovoltaic Generators," *IEEE Transactions on Smart Grid,* vol. 5, pp. 2718-2728, Nov 2014.

[6] N. Daratha, B. Das, and J. Sharma, "Coordination Between OLTC and SVC for Voltage Regulation in Unbalanced Distribution System Distributed Generation," *IEEE Transactions on Power Systems,* vol. 29, pp. 289-299, Jan 2014.

[7] R. A. Jabr and I. Dzafic, "Sensitivity-Based Discrete Coordinate-Descent for Volt/VAr Control in Distribution Networks," *IEEE Transactions on Power Systems,* pp. 1-9, 2016.

[8] P. Sulc, S. Backhaus, and M. Chertkov, "Optimal Distributed Control of Reactive Power Via the Alternating Direction Method of Multipliers," *IEEE Transactions on Energy Conversion,* vol. 29, pp. 968-977, 2014.

[9] B. Zhang, A. Y. S. Lam, A. D. Dominguez-Garcia, and D. Tse, "An Optimal and Distributed Method for Voltage Regulation in Power Distribution Systems," *IEEE Transactions on Power Systems,* vol. 30, pp. 1714-1726, 2015.

[10] E. Bullich-Massagué, O. Gomis-Bellmunt, L. Serrano-Salamanca, *et al*, "Power plant control in large-scale photovoltaic plants: design, implementation and validation in a 9.4 MW photovoltaic plant," *IET Renewable Power Generation,* vol. 10, pp. 50-62, 2016.

[11] *Power Generation Systems Connected to the Low/Voltage Dstribution Network,* VDE-AR-N 4105:2011-08, Forum Netztechnik/Netzbetriebim VDE (FNN), Berlin, Germany, 2011.

[12] A. Samadi, R. Eriksson, L. Soder, *et al*, "Coordinated Active Power-Dependent Voltage Regulation in Distribution Grids With PV Systems," *IEEE Transactions on Power Delivery,* vol. 29, pp. 1454-1464, Jun 2014.

[13] K. Turitsyn, P. Sulc, S. Backhaus, and M. Chertkov, "Options for Control of Reactive Power by Distributed Photovoltaic Generators," *Proceedings of the IEEE,* vol. 99, pp. 1063-1073, Jun 2011.

[14] D. S. E. Demirok, R. Teodorescu, K.H.B. Frederiksen "An Optimized Local Reactive Power Control for High Penetration of Distributed Solar Inverters in Low Voltage Networks," presented at the 26th European Photovoltaic Solar Energy Conference and Exhibition Hamburg, 2011.

[15] B. Bletterie, S. Kadam, R. Bolgaryn, and A. Zegers, "Voltage control with PV inverters in low voltage networks – In depth analysis of different concepts and parameterization criteria," *IEEE Transactions on Power Systems,* pp. 1-1, 2016.

[16] S. Weckx, C. Gonzalez, and J. Driesen, "Combined Central and Local Active and Reactive Power Control of PV Inverters," *IEEE Transactions on Sustainable Energy,* vol. 5, pp. 776-784, 2014.

[17] Energex Limited (Energex), The University of Queensland (Customer). *Negotiated Customer Connection Contract (without construction, with generator embedded within customer network*. Available: https://www.gci.uq.edu.au/filething/get/6363/NCC-without-Construction-with-Generator-Embedded_v5_Executed%20201114-Technical%20Extract-8.pdf

[18] V. Garrone, M. Hibbert, J. Mayer, "Technical Requirements for the Connection of a MW-scale PV Array with Battery Storage to an 11kV Feeder in Queensland," *Asia-Pacific Solar Research Conf.*, 2014.

[19] C. Trueblood, S. Coley, T. Key, *et al.*, "PV Measures Up for Fleet Duty : Data from a Tennessee Plant Are Used to Illustrate Metrics That Characterize Plant Performance," *IEEE Power and Energy Magazine,* vol. 11, pp. 33-44, 2013.

[20] AS 2279.4: 'Australian Standard – Disturbances in mains supply networks – limitation of voltage fluctuations caused by industrial equipment', 1991.

[21] Kersting, W.H.: "Distribution system modelling and analysis," (The Electric Power Engineering Series, 2007, 2nd edn.)

[22] P. Jahangiri and D. C. Aliprantis, "Distributed Volt/VAr Control by PV Inverters," *IEEE Transactions on Power Systems,* vol. 28, pp. 3429-3439, 2013.

Licheng Wang (S'2016) completed his B.Sc from Huazhong University of Science and Technology in 2012, and completed his M.Sc from Zhejiang University in 2015. Currently, he is a PhD student in the Power & Energy Systems Research Division at the School of Information Technology and Electrical Engineering, the University of Queensland, Australia. His research interest is renewable energy integration in distribution systems.

Ruifeng Yan (S'2009, M'2012) received the B. Eng. (Hons.) degree in Automation from University of Science and Technology, Beijing, China, in 2004, the M. Eng degree in Electrical Engineering from the Australian National University, Canberra, Australia, in 2007, and Ph.D. degree in Power and Energy Systems from the University of Queensland, Brisbane, Australia, in 2012. His research interests include power system operation and analysis, and renewable energy integration into power networks.

Tapan Kumar Saha (M'93, SM'97) was born in Bangladesh in 1959 and immigrated to Australia in 1989. He received his B. Sc. Engineering (electrical and electronic) in 1982 from the Bangladesh University of Engineering & Technology, Dhaka, Bangladesh, M. Tech (electrical engineering) in1985 from the Indian Institute of Technology, New Delhi, India and PhD in 1994 from the University of Queensland, Brisbane, Australia. Tapan is currently Professor of Electrical Engineering in the School of Information Technology and Electrical Engineering, University of Queensland, Australia. Previously he has had visiting appointments for a semester at both the Royal Institute of Technology (KTH), Stockholm, Sweden and at the University of Newcastle (Australia). He is a Fellow of the Institution of Engineers, Australia. His research interests include condition monitoring of electrical plants, power systems and power quality.